An Anisotropic Multi-front Fast Marching Method for Real-Time Simulation of Cardiac Electrophysiology

Maxime Sermesant[1,2], Ender Konukoğlu[1], Hervé Delingette[1], Yves Coudière[4], Phani Chinchapatnam[3], Kawal S. Rhode[2], Reza Razavi[2], and Nicholas Ayache[1]

[1] INRIA Sophia Antipolis, Asclepios Team, France
[2] King's College London, Division of Imaging Sciences, UK
[3] University College London, Centre for Medical Image Computing, UK
[4] Nantes University, Jean Leray Mathematics Laboratory, France

Abstract. Cardiac arrhythmias can develop complex electrophysiological patterns which complexify the planning and control of therapies, especially in the context of radio-frequency ablation. The development of electrophysiology models aims at testing different therapy strategies. However, current models are computationally expensive and often too complex to be adjusted with limited clinical data. In this paper, we propose a real-time method to simulate cardiac electrophysiology on triangular meshes. This model is based on a multi-front integration of the Fast Marching Method. This efficient approach opens new possibilities, including the ability to directly integrate modelling in the interventional room.

1 Introduction

Treatment of cardiac arrhythmias has considerably changed in the last decades. Radio-frequency ablation techniques are becoming widely available as an alternative to drug therapy. These procedures can be highly effective with minimal side effects, but for some groups of patients have unsatisfactory success rates, may entail long procedures, and may involve high x-ray radiation dose to both patient and staff. Moreover, serious side effects can arise if the lesions extend beyond the target area. There is a need for substantial innovation in order to reliably achieve successful results in an acceptable time, with lower radiation dose and reduced risk of accidental damage to adjacent structures.

The aim of this research work is to design models of the cardiac electrophysiology that are suited for clinical use and to propose methods to combine these models with interventional data in order to better estimate the patient cardiac function and help in the guidance of procedures.

2 Electrophysiology Models

Modelling the cell electrophysiology is an active research area since the seminal work of Hodgkin and Huxley [4]. The precise modelling of the myocardium

F.B. Sachse and G. Seemann (Eds.): FIMH 2007, LNCS 4466, pp. 160–169, 2007.
© Springer-Verlag Berlin Heidelberg 2007

involves a cell membrane model embedded into a set of partial differential equations (PDE) modelling a continuum. We can divide these models into three categories, from the more complex to the simpler (numerically):

- Biophysical models: semi-linear evolution Partial Differential Equation (PDE) with ionic models. Up to fifty equations for ion concentrations and channels [9,10]
- Phenomenological models: semi-linear evolution PDE with mathematical simplification of biophysical models. Reducing to two equations representing the intra- and extra-cellular potentials (bi-domain, mono-domain [2,11])
- Eikonal models: one static non-linear PDE for the depolarisation time derived from the previous models (Eikonal-Curvature [6], Eikonal-Diffusion [3])

Solutions of the evolution PDE are very computationally demanding, due to the space scale of the electrical propagation front being much smaller than the size of the ventricles. The motion of the front governed by the Eikonal equation is observed at a much larger scale, resulting in much faster computations.

For our interventional purpose, and as parameter adjustment often requires several simulations, we want to design a very fast model. Moreover, clinical data currently available is mainly on depolarisation times. For these reasons we chose to base the presented work on the Eikonal models. Even if these models are not able to precisely simulate the whole range of cardiac pathologies, they open up possibilities for fast estimation, filtering (smoothing), interpolation and extrapolation.

In [14], we presented an approach to simulate the Eikonal models with a Fast Marching Method (FMM), in order to obtain very fast computations. While this approach allowed us to take the front curvature influence into account, we could not integrate the repolarisation in this approach. However, the repolarisation is a very important phenomenon in many arrhythmias, for instance when the Action Potential Duration (APD) variation creates reentry waves. Moreover, it is often over several cycles that arrhythmias develop, and the FMM only solves for separate cycles. Finally, this approach could not cope with the anisotropy of the heart.

In this article we propose two important contributions in this fast model framework. First, we propose a FMM that takes into account the anisotropy of the medium in the computation of the propagation. Second, we introduce the repolarisation phenomenon in order to be able to simulate multi-front propagations.

3 The Anisotropic Fast Marching Method

3.1 The Fast Marching Method (FMM)

We first compare briefly the Eikonal approach to the PDE one. The classical FMM [16] can be used to solve the following isotropic Eikonal equation:

$$F\sqrt{\nabla T^t \nabla T} = 1$$

where T is the arrival time and F the speed function (D is the identity matrix in the isotropic case). In this method, points are separated in three sets: $UNKNOWN$, $TRIAL$, and $KNOWN$, and the $TRIAL$ set of points X is ordered along the increasing associated times $T(X)$. $\mathcal{N}(X)$ is the neighbourhood of X. In the initialisation step, all the points are put in $UNKNOWN$ with a time of $+\infty$, starting points are put in $KNOWN$ with a time of 0, and their neighbours are updated. The FMM algorithm is described briefly in Algorithms 1 and 2.

Algorithm 1. Fast Marching Method

while TRIAL list is not empty **do**
  $X \leftarrow \text{argmin}_{X \in TRIAL}\{T(X)\}$
  remove X from $TRIAL$ and add X to $KNOWN$
  for all $X_i \in \mathcal{N}(X)$ and $X_i \notin KNOWN$ **do**
    compute $T(X_i) = \text{UPDATE}(X_i, X)$
    if $X_i \notin TRIAL$ then add X_i to $TRIAL$
  end for
end while

Algorithm 2. Computation of $\overline{T}(X_i) = UPDATE(X_i, X)$ in a Triangulation

$\overline{T}(X_i) \leftarrow +\infty$
for all $\triangle(XX_iY) \in \triangle^X_{X_i} = \{\triangle(XX_iY) | Y \in \mathcal{N}(X_i)\}$ **do**
  if $Y \in KNOWN$ **then**
    $\overline{T}(X_i) \leftarrow \min\{\overline{T}(X_i), \min_{p\in[0,1]}(T(X)p + T(Y)(1-p) + [\mathbf{v}(p)^t D^{-1}\mathbf{v}(p)]^{1/2}/F)\}$
    where $\mathbf{v}(p) = \overrightarrow{XX_i}p + \overrightarrow{YX_i}(1-p)$
  else
    $\overline{T}(X_i) \leftarrow \min\{\overline{T}(X_i), T(X) + \overrightarrow{XX_i}^t D^{-1}\overrightarrow{XX_i}\}$
  end if
end for

This implementation of the FMM is different from the original one which uses an upwind discretisation of the gradient. We use here a closed-form solution of the minimisation in triangles, which seems to be less sensitive to obtuse angles than the original FMM (this has to be further studied.).

The Eikonal equation can be seen as an approximation for the computation of the propagating front from reaction-diffusion PDEs. To better understand the approximation, we present in Fig. 1 a comparison of the isochrones computed by the FMM and the Aliev and Panfilov reaction-diffusion system to simulate cardiac action potential [1]. The results from the different algorithms are presented on a triangulated square mesh with a center hole, composed of 13 000 nodes. The initialisation is in the bottom left corner. In this isotropic case, D is the identity matrix.

In this case, the isochrones of the FMM are close to what is produced by the PDE. One main difference is related to the boundary conditions. For the PDE,

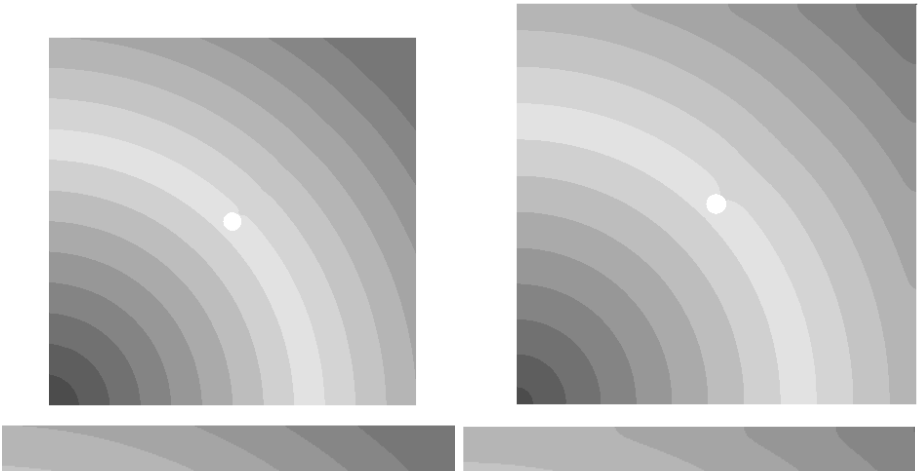

Fig. 1. (Left) Fast Marching on unstructured grid, (right) isochrones from the simulated PDE. Red corresponds to small times, blue to large times. (Bottom) close up on the top of the square to point out boundary condition differences effect.

these are Neumann boundary conditions, which impose the no-flux condition at the boundary, whereas the Eikonal equation has no such constraints. This is visible for instance at the top and right boundaries, where the PDE front is orthogonal to the edge and not the Eikonal one (see Fig. 1, bottom row, and around the central hole). There are ways to introduce this in the Eikonal approach, but this is still on going work on what are the proper boundary conditions for our case, and whether this will impact the simulation to a great extent.

Another difference can arise from the fact that the travelling wave solution of the PDE is only an asymptotic solution, whereas the Eikonal solution is directly in this stationnary state. This can be seen by varying the initialisation parameters of the PDE (shape of the front at the initial time).

The travelling wave solution to the PDE is an asymptotic state (as time tends to $+\infty$), whose isochrones are approximately solutions to the Eikonal equation (neglecting the effect of front curvature). Hence, part of the error between the PDE isochrones and the Eikonal solution arises from the transient propagation when the initial data for the PDE is chosen far from the asymptotic state.

The PDE system models a wide range of functional states (plane/spiral waves, relations between front curvature, local APD and speed, adaptive response to a periodic stimulation, etc), with the counterpart of complex parameter tuning and numerical stability/cost issues. Although accounting for simpler situations, the Eikonal model is clearly more adapted to our concern: fast computing compared to very sparse/local measurements.

A more precise and quantitative evaluation of both the modeling and the numerical approximation errors is on-going work.

3.2 The Anisotropic Fast Marching

The anisotropic Eikonal equation can be written in the form of:

$$F\sqrt{\nabla T^t D \nabla T} = 1$$

where D is the tensor creating anisotropy. Taking into account the anisotropy of the propagation is important in many cases of excitable media. But introducing this phenomenon in the FMM is not trivial. Indeed, the regular FMM uses the collinearity between the gradient and the characteristic direction to solve the equation very efficiently, but in the anisotropic case these directions do not match anymore.

There have been many different ways proposed to solve such anisotropic equations using single-pass [15,7] or iterative [5,12] methods. We use here a new fast algorithm for solving anisotropic Eikonal equation on general meshes without increasing the neighborhood and following the characteristic direction similar to single-pass methods [8]. The idea is to include a recursive correction scheme taking into account the fact that, due to anisotropy, the immediate neighborhood used for computation may not always contain the characteristic direction at the time it is computed. To achieve this, an additional $CHANGED$ list who is also empty at the beginning and who will be used for the recursive correction is introduced. This efficient algorithm, described in Algorithm 3, can cope with very important anisotropies and can be applied to more general forms of static convex Hamilton-Jacobi equations, and on Cartesian or unstructured grids. The anisotropic FMM algorithm is not significantly longer to compute than the classical algorithm, especially in the case of non-extreme anisotropies. For instance with a factor of three between longitudinal and transverse speeds, simulation on the 13 000 nodes took less than one second (see Fig. 2).

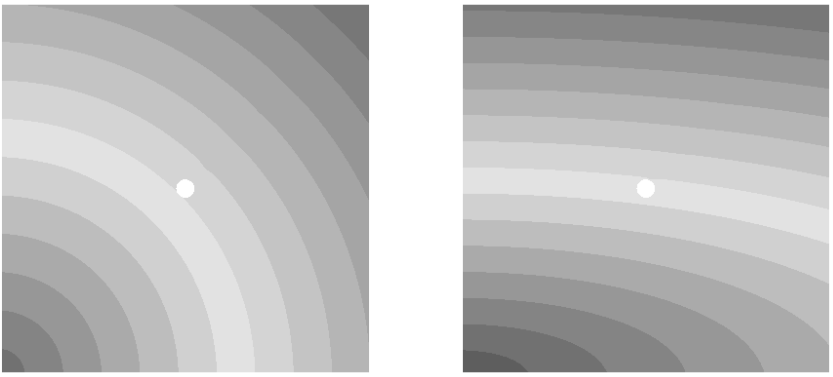

Fig. 2. (Left) Classical Fast Marching on unstructured grid, (right) Anisotropic Fast Marching (different colormap). The vertical speed is three times smaller than the horizontal speed.

Algorithm 3. Anisotropic Fast Marching

```
while TRIAL or CHANGED are not empty do
  if CHANGED is not empty then
    X ← argmin_{X∈CHANGED}{T(X)}
    remove X from CHANGED
  else
    X ← argmin_{X∈TRIAL}{T(X)}
    remove X from TRIAL and add X to KNOWN
  end if
  for all X_i ∈ N(X) and X_i ∈ KNOWN do
    compute T̄(X_i) = UPDATE(X_i, X)
    if T̄(X_i) < T(X_i) then
      T(X_i) ← T̄(X_i)
      add X_i to CHANGED list
    end if
  end for
  for all Y_i ∈ N(X) and Y_i ∈ TRIAL ∪ UNKNOWN do
    compute T̄(Y_i) = UPDATE(Y_i, X)
    if Y_i ∈ TRIAL and T̄(Y_i) < T(Y_i) then
      T(Y_i) ← T̄(Y_i)
    else if Y_i ∈ UNKNOWN then
      T(Y_i) ← T̄(Y_i)
      remove Y_i from UNKNOWN and add Y_i to TRIAL
    end if
  end for
end while
```

4 A Multi-front Fast Marching Approach

The FMM is a static method to solve for an evolving front, in the sense that the variable of the Eikonal equation is time. But in our simulation purpose, we can have several fronts evolving at the same time, because points can go back to a resting state, so they can be excited again before the first front disappeared.

The key idea is to introduce a time-stepping scheme while using the FMM to compute the propagation during each time step. Our application context is the Eikonal approximation of reaction-diffusion equations to simulate the propagation in excitable media. In this context, the state of each point may vary over time, for instance with a repolarisation state, when a point goes back to its equilibrium state.

In order to achieve this, we have to introduce a refractory state, between the excited and the equilibrium state, otherwise, any node going back to the equilibrium would immediately be excited again by his neighbours still excited. This is in agreement with natural phenomena, like nervous electrical action potential propagation, where cells have this refractory period. The Multi-Front FMM is described in algorithm 4.

Algorithm 4. Multi-Front Fast Marching Algorithm on a period T

```
integratedTime = 0.0
while integratedTime < T do
  elapsedTime = 0.0
  while TRIAL not empty and elapsedTime < timeStep do
    X ← argmin_{X∈TRIAL}{T(X)}
    remove X from TRIAL and add X to KNOWN
    for all X_i ∈ N(X) and X_i ∉ KNOWN do
      compute T(X_i) = UPDATE(X_i, X)
      if X_i ∉ TRIAL then add X_i to TRIAL
      elapsedTime = T(X_i) − integratedTime
    end for
    for all X ∈ KNOWN do
      if elapsedTime − T(X) > APD(X) then
        remove X from KNOWN and add X to REFRACTORY
        RepolarisationTime(X) ← T(X) + APD(X)
      end if
    end for
    for all X ∈ REFRACTORY do
      if elapsedTime − RepolarisationTime(X) > RefractoryPeriod(X) then
        remove X from REFRACTORY and add X to UNKNOWN
      end if
    end for
  end while
  integratedTime += timeStep
end while
```

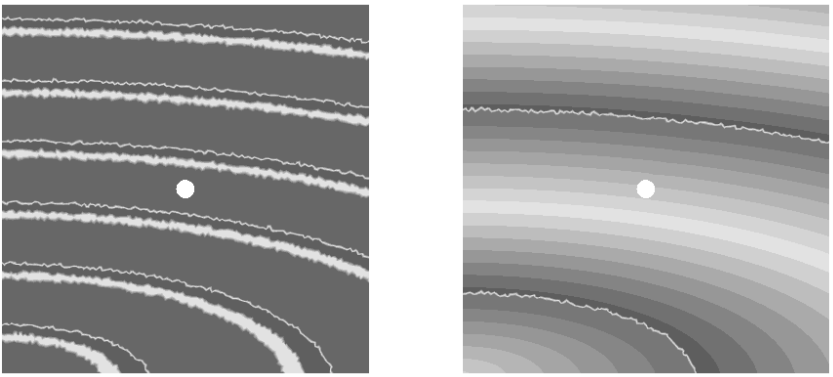

Fig. 3. (Left) Impulse train with the Multi-Front Fast Marching (anisotropic case). Excited vertices are in red and refractory vertices are in yellow. (Right) Corresponding isochrones with a reduced frequency to increase visibility.

This Multi-Front FMM is able to simulate an impulse train on a piece of excitable media (see Fig. 3, left). The visualised progressing front is not very

smooth, because it corresponds to an isochrone still being computed, but after the front, the resulting isochrones are smooth (see Fig. 3, right). Visualisation work still has to be made to improve this.

The computation speed can be adjusted by choosing the frequency at which the display must be updated (corresponding to the "time step" in this scheme). On recent computers and with smaller meshes (1000 nodes), such surface simulations could be done in "real-time": no synchronisation was done to ensure the timing of the simulation, but it was visually checked that with 30 frames per cycle, the computation time was below one second (one heart cycle is a bit less than a second).

5 Cardiac Electrophysiology Simulation

The presented algorithm was used to simulate transmembrane potential propagation in cardiac tissue. The idea is to compute the depolarization time using the Multi-Front Anisotropic FMM. Then, when a given vertex is depolarised, we use the time-stepping to know when the vertex goes into repolarisation and then refractory period, and when it is excitable again. We can thus show a pseudo transmembrane potential, which is at 10 mV when the vertex is depolarised (red), and -90 mV when it is excitable (blue).

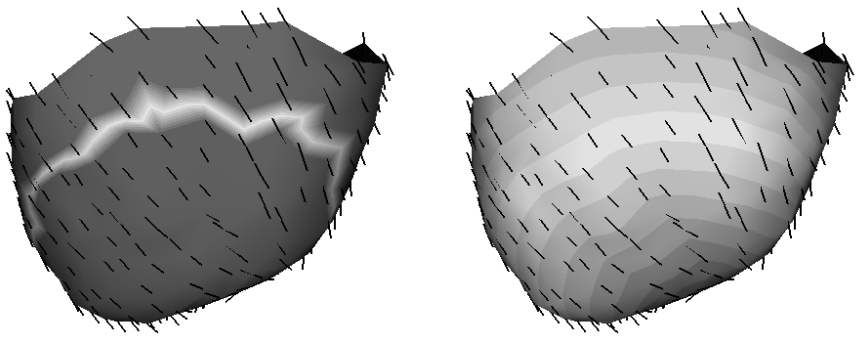

Fig. 4. Normal propagation on the epicardium, with an apical epicardial pacing. Black lines represent the fibre orientations. (Left) pseudo transmembrane potential. (Right) simulated isochrones.

We compute in a continuous way the propagation of different finite states. Compared to previous approaches in propagation simulation, it could be seen as a kind of "continuous cellular automaton": the states are discrete but the propagation is continuous.

We used this algorithm to simulate epicardial propagation of the Action Potential. As fibre orientation is tangential on the epicardium, and we simulate an epicardial pacing, this surface model can be seen as an approximation of the 3D

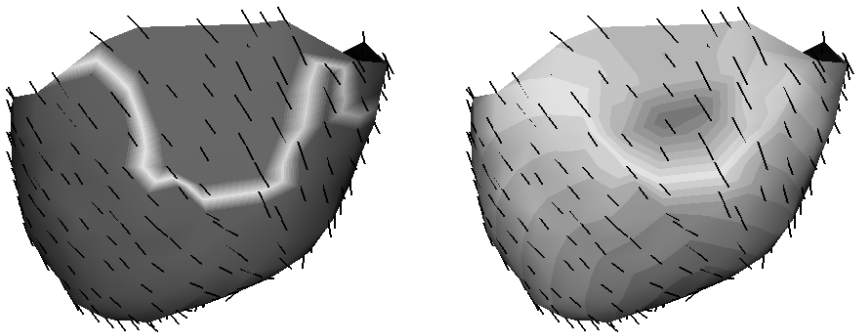

Fig. 5. Simulation of a scar with 10% of normal conductivity. Black lines represent the fibre orientations. (Left) pseudo transmembrane potential. (Right) simulated isochrones.

propagation (see Fig. 4). We integrate fibre orientations from DTI measurements. The depolarisation speed is 3 times faster along the fibre than transversally.

Low conductivity areas can also be added. For instance, a scarred area created with a conductivity of 10% of the normal conductivity was simulated, see Fig. 5.

These are just exemplar simulations, computed on a very crude mesh (248 points). The accurate simulation of arrhythmias needs to take into account the full 3D nature of the propagation and deal carefully with any discretisation approximation issues. We also need a thorough comparison between measured isochrones and simulated ones from a PDE or Fast Marching approach for pathological cases in order to fully validate the behaviour of these models.

6 Conclusion

We presented a new algorithm to achieve real-time simulations of cardiac electrophysiology. This model opens up possibilities for real-time filtering and interpolation of sparse and noisy catheter-based electrophysiology recordings, which could provide a better evaluation of pathology and planning of the therapy. An excellent example application is the planning of radio-frequency ablation. Such a real-time model could be embedded in an intervention simulator to test several ablation strategies.

Future work includes extension to volumetric propagation and reintroducing the influence of the curvature of the front on the propagation speed. The use of a restitution curve is quite straightforward in this framework, but having a relative refractory period will need a more precisely described action potential. Visualisation can be improved in order to have a smoother front by using already computed isochrones. Validation of this model should lead to the integration of simulated isochrones within XMR interventional data, that combine patient anatomy and electrophysiology mapping [13].

References

1. Aliev, R., Panfilov, A.: A simple two-variable model of cardiac excitation. Chaos, Solitons and Fractals 7(3), 293–301 (1996)
2. FitzHugh, R.: Impulses and physiological states in theoretical models of nerve membrane. Biophysical Journal 1, 445–466 (1961)
3. Colli Franzone, P., Guerri, L., Rovida, S.: Wavefront propagation in activation model of the anisotropic cardiac tissue: Asymptotic analysis and numerical simulations. J. Math. Biol. (1990)
4. Hodgkin, A., Huxley, A.: A quantitative description of membrane current and its application to conduction and excitation in nerve. Journal of Physiology 177, 500–544 (1952)
5. Kao, C., Osher, S., Tsai, Y.: Fast sweeping methods for static hamilton-jacobi equations. SIAM J. Numer. Anal. 42 (2005)
6. Keener, J., Sneyd, J.: Mathematical Physiology. Springer, Heidelberg (1998)
7. Kevorkian, J.: Partial differential equations: Analytical solution techniques. Springer, Heidelberg (2000)
8. Konukoğlu, E., Sermesant, M., Peyrat, J-M., Clatz, O., Delingette, H., Ayache, N.: A recursive anisotropic fast marching approach to reaction diffusion equation: Application to tumor growth modeling. In: Information Processing in Medical Imaging (IPMI'07). LNCS, Springer, Heidelberg, Accepted (2007)
9. Luo, C., Rudy, Y.: A model of the ventricular cardiac action potential: depolarization, repolarization, and their interaction. Circulation Research 68, 1501–1526 (1991)
10. Noble, D., Varghese, A., Kohl, P., Noble, P.: Improved guinea-pig ventricular cell model incorporating a diadic space, I_{Kr} and I_{Ks}, and length and tension dependent processes. Canadian Journal of Cardiology 14, 123–134 (1998)
11. Pollard, A., Hooke, N., Henriquez, C.: Cardiac propagation simulation. Critical Reviews in biomedical Engineering 20(3,4), 171–210 (1992)
12. Qian, J., Zhang, Y., Zhao, H.: A fast sweeping method for static convex hamilton-jacobi equations. UCLA Computational and Applied Mathematics Reports, 06-37 (2006)
13. Rhode, K., Sermesant, M., Brogan, D., Hegde, S., Hipwell, J., Lambiase, P., Rosenthal, E., Bucknall, C., Qureshi, S., Gill, J., Razavi, R., Hill, D.: A system for real-time XMR guided cardiovascular intervention. IEEE Transactions on Medical Imaging 24(11), 1428–1440 (2005)
14. Sermesant, M., Coudière, Y., Moreau-Villéger, V., Rhode, K.S., Hill, D.L.G, Ravazi, R.: A fast-marching approach to cardiac electrophysiology simulation for XMR interventional imaging. In: Duncan, J.S., Gerig, G. (eds.) MICCAI 2005. LNCS, vol. 3750, pp. 607–615. Springer, Heidelberg (2005)
15. Sethian, J., Vladimirsky, A.: Ordered upwind methods for static hamilton-jacobi equations: theory and algorithms. SIAM J. Numer. Anal. 41 (2003)
16. Sethian, J.A.: Level set methods and fast marching methods: Evolving interfaces in computational geometry, fluid mechanics, computer vision, and materials science. Cambridge University Press, Cambridge (1999)